Molecular Systems Biology 8; Article number 626; doi:10.1038/msb.2012.57
Citation: ***Molecular Systems Biology*** **8:626**

www.molecularsystemsbiology.com

molecular systems biology

Programming stress-induced altruistic death in engineered bacteria

Yu Tanouchi[1], Anand Pai[1], Nicolas E Buchler[2,3,4,5] and Lingchong You[1,4,5,*]

[1] Department of Biomedical Engineering, Duke University, Durham, NC, USA, [2] Department of Physics, Duke University, Durham, NC, USA, [3] Department of Biology, Duke University, Durham, NC, USA, [4] Center for Systems Biology, Duke University, Durham, NC, USA and [5] Institute for Genome Sciences and Policy, Duke University, Durham, NC, USA

* Corresponding author. Department of Biomedical Engineering, Duke University, CIEMAS 2355 101, Science Drive, Box 3382, Durham, NC 27708, USA. Tel.: +1 919 660 8408; Fax: +1 919 668 0795; E-mail: you@duke.edu

Received 3.5.12; accepted 9.10.12

Programmed death is often associated with a bacterial stress response. This behavior appears paradoxical, as it offers no benefit to the individual. This paradox can be explained if the death is 'altruistic': the killing of some cells can benefit the survivors through release of 'public goods'. However, the conditions where bacterial programmed death becomes advantageous have not been unambiguously demonstrated experimentally. Here, we determined such conditions by engineering tunable, stress-induced altruistic death in the bacterium *Escherichia coli*. Using a mathematical model, we predicted the existence of an optimal programmed death rate that maximizes population growth under stress. We further predicted that altruistic death could generate the 'Eagle effect', a counter-intuitive phenomenon where bacteria appear to grow better when treated with higher antibiotic concentrations. In support of these modeling insights, we experimentally demonstrated both the optimality in programmed death rate and the Eagle effect using our engineered system. Our findings fill a critical conceptual gap in the analysis of the evolution of bacterial programmed death, and have implications for a design of antibiotic treatment.
Molecular Systems Biology **8:** 626; published online 20 November 2012; doi:10.1038/msb.2012.57
Subject Categories: synthetic biology; microbiology & pathogens
Keywords: altruistic death; antibiotic response; eagle effect; programmed cell death; synthetic biology

Introduction

Programmed death is commonly associated with bacterial response to stressful conditions, such as amino-acid starvation (Aizenman *et al*, 1996), presence of competitors (Ackermann *et al*, 2008), and antibiotic treatment (Rice and Bayles, 2003; Hazan *et al*, 2004). As death offers no benefit to its actor (i.e., a bacterial cell that has activated programmed death will die), its occurrence raises a fundamental, unresolved question with regard to its evolution: how can this trait be selected for? An oft-cited explanation is that the death is 'altruistic': the killing of some cells can provide direct or indirect benefits to the survivors, including the actor's kin, through the release of 'public goods' (Figure 1A) (West *et al*, 2007). In other words, death may represent an extreme form of cooperation, analogous to sterile workers in social-insect colonies who give up their personal reproduction but benefit their fertile family members (Gardner and Kümmerli, 2008). By making this assumption, evolution of programmed death in microbes can be analyzed under the general framework of public-good cooperation (Ackermann *et al*, 2008). Figure 1A summarizes several natural examples that may fit in this framework: *Streptococcus pneumoniae* (Berry *et al*, 1989; Hirst *et al*, 2004) responds to its host environment and releases the virulence factor pneumolysin through cell lysis, which helps its host invasion. *Salmonella typhimurim* (Stecher *et al*, 2007; Ackermann *et al*, 2008) responds to competition in the host's microbiota by causing host inflammation through programmed death. This inflammation kills the microbiota and reduces competition. *E. coli* (Aizenman *et al*, 1996) responds to amino-acid starvation by triggering programmed death, which is speculated to help surviving cells by providing nutrients. Colicinogenic *E. coli* responds to DNA-damaging agent and nutrient depletion by releasing colicin through cell lysis, which kills neighboring competitors (Gardner *et al*, 2004; Cascales *et al*, 2007). In response to nutrient limitation, *Bacillus subtilis* develops spores, an extreme means to withstand the stress. *B. subtilis* delays the sporulation by killing and feeding on their non-sporulating siblings to prevent unnecessary spore formation in case the environmental condition improves shortly (Ellermeier *et al*, 2006). Other examples of possible public goods resulting from programmed death include extracellular DNA, a structural component of biofilm in *Pseudomonas aeruginosa* (Allesen-Holm *et al*, 2006), *Staphylococcus aureus* (Rice *et al*, 2007), and *Streptococcus mutants*.

While plausible, however, the conditions where altruistic death becomes advantageous have not been unequivocally

A Conceptual framework

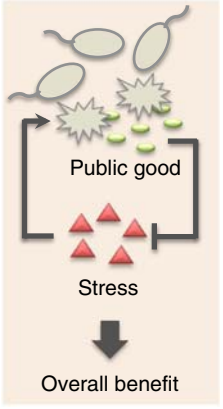

Organism	Stress	Public good	Overall benefit
S. pneumoniae	Host environment	Pneumolysin	Invasion
S. typhimurium	Host environment/ competition with microbiota	Host inflaimmation	Colonization
E. coli	Amino-acid starvation	Nutrient	Survival
E. coli	DNA damage/ starvation	Colicin	Reduced competition
B. subtilis	Starvation	Nutrient	Delay in sporulation

B

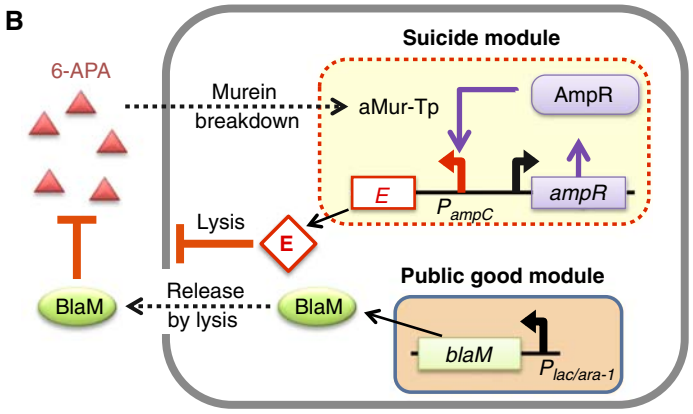

Figure 1 Altruistic bacterial death in response to stress. (**A**) Coupling programmed death with public-good production. Some cells undergo programmed death in response to stress (red triangles), leading to generation of a public good (green ovals). The public good removes the stress, allowing survival and recovery of the overall population. Table: examples of natural systems where programmed bacterial death has been proposed to be altruistic by providing direct or indirect benefits to survivors. See text for further details. (**B**) A synthetic gene circuit to program altruistic death. 6-APA causes murein breakdown and generates aMur-Tp inside the cell; aMur-Tp induces expression of the *E* gene by activating the P_{ampC} promoter through AmpR. A non-secreted form of beta-lactamase (BlaM) is placed under IPTG-inducible promoter, $P_{lac/ara-1}$. Upon cell lysis owing to E expression, BlaM is released to the extracellular space where it degrades 6-APA. In the conceptual framework described in (A), 6-APA represents the stress, whereas BlaM represents the public good.

demonstrated in an experimental system. As such, there remains a considerable gap between theoretical models and corresponding experimental validation. For example, a recent study of *S. typhimurim* used an evolutionary game theory approach to investigate conditions under which evolution of altruistic death is possible (Ackermann *et al*, 2008). It demonstrated that basic assumptions of the altruistic-death model are consistent with experiments, but the exact nature of cost–benefit relationship of death remains elusive. A major challenge in tackling this problem is the complexity of natural biological processes, where confounding factors could obscure the quantitative analysis and interpretation of the outcome resulting from the trade-off between death and public-good production. These include the severity of initial stress, degree of death, per-cell rate of public-good generation, as well as the growth cycle of the organism. Often times, precise manipulation and even interpretation of basic parameters are nearly impossible. For instance, during *S. typhimurium* infection, the benefit results from a combination of highly intertwined, host–pathogen–microflora interactions (Stecher *et al*, 2007; Ackermann *et al*, 2008) while the system responsible for suicide (type-III secretion system) have multiple roles in pathogenesis (Haraga *et al*, 2008). Modifying one factor likely has diverse and unintended effects; thus the experimental results are open to alternative explanations (Nedelcu *et al*, 2011).

Owing to these issues, it remains an open question with regard to the specific conditions under which programmed death can pay off at the population level. To address this question, we have taken a synthetic-biology approach to explicitly measure and test the adaptive advantage of programmed bacterial death through the release of public goods. We created synthetic gene circuits in *E. coli* that respond to environmental stress by exhibiting varying extent of programmed death that releases a public good (Figure 1B). In our circuits, both the degree of programmed death and the rate of public-good production are tunable, which allows us to test the benefits of altruistic death under various conditions in a controllable manner.

Such synthetic systems are often simpler than their natural counterparts, have fewer confounding factors, are amenable to modulation of system parameters, and allow clear mapping

between experimental manipulation and its effect (Tanouchi *et al*, 2009). This approach has been successfully adopted to investigate other problems of population and evolutionary biology, and is complementary to directly studying natural systems (Kerr *et al*, 2002; Shou *et al*, 2007; Acar *et al*, 2008; Chuang *et al*, 2009, 2010; Song *et al*, 2009). For instance, Chuang *et al* (2009) created a secretion-based cooperation system in *E. coli* where 'producers' secrete a public good at the cost of reduced growth rate whereas 'non-producers' benefit from the public good without paying the cost. Using this system, the authors studied how population structure, cost of being the producer, and degree of benefit affect the outcome of competition between the two strains (Chuang *et al*, 2009). In this study, we have used a similar approach to address an unresolved, more complex biological phenomenon, namely altruistic death where cells completely give up their reproductive opportunity upon public-good production.

Using our synthetic system, we examined whether altruistic death can promote population fitness, and elucidated how this fitness depends on intrinsic (e.g., production rate of the public good and the programmed death rate) and extrinsic (e.g., the stress level, duration, and cell density at which the stress is applied) factors. Our approach also revealed a mechanistic explanation for the 'Eagle effect', a counter-intuitive phenomenon where bacteria appear to grow better when treated with higher antibiotic concentrations. This result provides a novel insight that connects two apparently unrelated phenomena, altruistic death and the Eagle effect. Overall, our results fill a conceptual gap in understanding the evolutionary dynamics of programmed bacterial death during stress and have implications for designing intervention strategies for effective treatment of bacterial infections.

Results

Circuit design, implementation, and parts characterization

Our base circuit, termed PAD (programmed altruistic death), consists of a suicide module and a public-good module (Figure 1B). The suicide module expresses the *E* lysis gene from bacteriophage φX174 under P_{ampC} promoter in response to a beta-lactam antibiotic, 6-APA. 6-APA causes partial cell-wall breakdown and accumulation of a cell-wall intermediate, anhMurNAc-tripeptide, which binds and activates AmpR, a transcriptional regulator of P_{ampC} promoter (Jacobs *et al*, 1997). The public-good module expresses a modified, cytoplasmic form of beta-lactamase (BlaM) from an IPTG-inducible promoter, $P_{lac/ara-1}$ (Lutz and Bujard, 1997). Having suicide function and public-good production in separate modules allows their independent modulation to examine their effects on system dynamics. That is, the BlaM production rate per cell can be modulated without the influence of the E protein production rate. Likewise, the death rate can be modulated by changing the translation rate of the E protein, for a given public-good production rate and stress level. Importantly, these changes can be mapped to separate parameters in our mathematical model (see below) in an unambiguous manner. As a control, we used a cell strain that is identical to PAD except that it lacks the *E* gene (no programmed death, or NPD). Microscope analysis confirmed significantly greater cell lysis for PAD in comparison with NPD (Supplementary Figure S1). It also suggested a minor growth inhibition effect of E protein for low *E* gene induction (i.e., low 6-APA concentration; Supplementary Figure S1d, e).

We chose BlaM for its two properties that are critical for the designed circuit function. First, because 6-APA recognizes its targets (penicillin-binding proteins) in the periplasm, a cytoplasmic BlaM should not protect cells against 6-APA (Broome-Smith and Spratt, 1986; Everett *et al*, 1990). We confirmed this idea experimentally by using a reporter circuit (pCSaGFP), where 6-APA-induced cell-wall damage is reported by GFP expression (Figure 2A). Our results showed that BlaM expression did not reduce the damage response in comparison with the negative control (without BlaM induction), indicating lack of 6-APA degradation. In contrast, the native, periplasmic form of beta-lactamase, Bla, reduced the damage response in comparision with the negative control (without Bla induction), indicating its ability to degrade 6-APA. Second, when released to extracellular space by cell lysis, BlaM should degrade 6-APA and offer protection for surviving cells. We tested this idea by using a protection assay (Figure 2B). Supernatant from lysed, BlaM-expressing cells offered full protection for a sensitive strain against 6-APA treatment. In contrast, supernatant from cells expressing BlaM but not lysed or that from lysed cells not expressing BlaM did not offer protection.

Therefore, the programmed death is completely altruistic by design in our circuits: the pubic good (BlaM) can only realize its protective function through the killing of its host cell. Also implied in this design is the requirement for cell–cell variability in death, which could arise from stochastic E protein expression or variable sensitivity to E-protein-mediated killing. We note that the first aspect is evident in the GFP expression from the P_{ampC} promoter in cells carrying a reporter circuit; the main peak of the GFP expression shows a broad distribution, covering about 50-fold range (Figure 2A).

Advantage of PAD at the population level

To test the advantage of altruistic death, we first compared growth dynamics of PAD and NPD in response to antibiotic treatment (Figure 3A). Altruistic death is defined to be advantageous when the PAD population outgrows the NPD population. Addition of 400 μg/ml 6-APA caused drastic lysis in the PAD strain but only slight lysis in the NPD strain. The density of the PAD strain remained lower than that of the NPD strain until ∼18 h later when it started to grow faster and eventually reached a higher density than the NPD strain. This growth advantage was due to faster release of BlaM and thus faster degradation of 6-APA (Figure 2B). This result provides a direct experimental demonstration that altruistic death can indeed benefit overall population survival in clonal populations, a minimum requirement for the evolution of altruistic death. The situation, however, is expected to reverse when the two strains are grown in a mixture. Social evolution theory predicts that a public-good producer (e.g., PAD) decreases in frequency when cocultured with a strain with no or less public-good production (e.g., NPD). Using

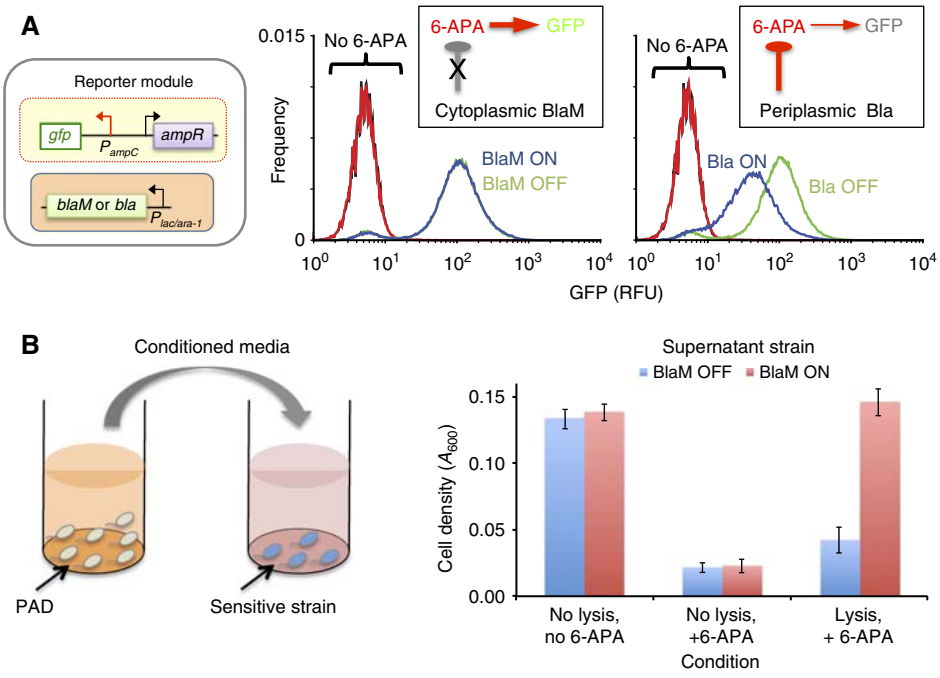

Figure 2 Characterization of the public-good module. (**A**) Cytoplasmic BlaM provides negligible protection against 6-APA. P_{ampC} induction upon 6-APA treatment was measured using GFP in relative fluorescence unit (RFU) in the presence of BlaM or Bla expression. BlaM expression (blue, induced by 1 mM IPTG) did not reduce GFP expression in comparison with negative control (green, no induction by IPTG), indicating that BlaM did not prevent cell-wall damage by 6-APA. In contrast, expression of the native Bla (blue, induced by 1 mM IPTG) reduced GFP expression in comparison with the negative control (green, no induction by IPTG). In the absence of 6-APA, GFP was not induced for either circuit, with (black) or without (red) 1 mM IPTG. (**B**) Released BlaM by cell lysis provides protection against 6-APA. Left: growth of a 6-APA-sensitive strain (lacking *E* gene and BlaM) was assayed in conditioned media containing supernatants prepared from PAD cultures with or without BlaM induction by 1 mM IPTG, and with (lysis) or without (no lysis) 6-APA treatment (400 μg/ml). Right: no lysis, no 6-APA (negative control): growth of the sensitive strain in the absence of 6-APA and in supernatants from unlysed PAD cultures. No lysis, + 6-APA: growth of the sensitive strain in supernatants from unlysed PAD cultures with 400 μg/ml 6-APA. Lysis, + 6-APA: growth of the sensitive strain in supernatants from PAD cultures lysed by 400 μg/ml 6-APA (i.e., 6-APA is present in the supernatants). Only supernatant from lysed PAD cells expressing BlaM provided significant protection for the sensitive strain against the 6-APA treatment. Error bars are s.d. of six replicates (three technical replicates × two independent experiments) for the growth assay.

fluorescence-tagged versions of PAD and NPD, we confirmed this prediction in our synthetic system (Supplementary Figure S2), thus reinforcing the idea that BlaM release by E-mediated cell lysis is altruistic and that BlaM is indeed a public good.

Furthermore, our circuits can serve as a well-defined model system to examine the interplay between critical parameters associated with altruistic death in response to stress. To this end, we developed a kinetic model for the programmed circuit dynamics (Equations (1)–(6), Supplementary Text, and Figure 3B). In the model, we focused on the effects of several experimentally tunable parameters, including the synthesis rate of the public good (β_2), the programmed death rate as modulated by the synthesis rate of the E protein (β_1), and the initial stress level (or 6-APA concentration, a). Other key determinants for the growth advantage of altruistic death are the time frame within which the growth dynamics are compared and the cell density at which programmed death is triggered. At earlier time points, altruistic death is detrimental as the population has not yet fully enjoyed the benefit of the released public good, the degradation of 6-APA (Figure 3A and B). Also, if programmed death was triggered at a low cell density, the public-good release would be low (limited by the total number of cells that can be possibly killed) and thus altruistic death would not become advantageous after the same duration of culturing (Supplementary Figure S3). These properties underscore the importance of factors defining the bacterial life cycle (initial density and growth duration) in determining the potential adaptive advantage of altruistic death. In subsequent analysis, our experimental growth dynamics were initialized with density of $A_{600} = 0.15$–0.2 and compared at 24 h post 6-APA treatment.

At a specific stress level, the rate of public-good production should affect the extent to which altruistic death can be advantageous for the population. This can be analyzed by varying the synthesis rate of BlaM. Indeed, for $a = 5.5$ at time zero, our model predicts that although increasing BlaM expression improve growth of both PAD and NPD strains, PAD strain is more fit than the NPD strain only when BlaM expression is sufficiently high ($\beta_2 > 3.6$) to compensate for the cost of death (Figure 3C). Consistent with the prediction, at 400 μg/ml 6-APA, increasing BlaM expression by IPTG enhanced overall growth, and the PAD strain outgrew the NPD strain only for IPTG greater than 0.25 mM (Figure 3D, Supplementary Figure S4). Thus, public-good release needs to be sufficiently high for altruistic death to be advantageous.

Prediction and validation of optimal death rates

Everything else being equal, the degree of programmed death should dictate the maximum net benefit of altruistic

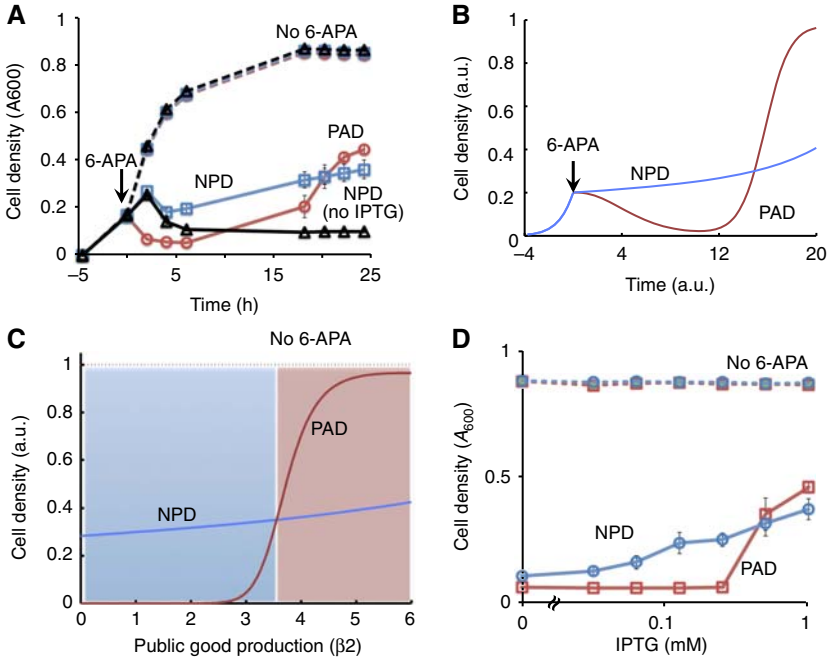

Figure 3 Emergence of growth advantage by PAD. (**A**) Growth dynamics of PAD (red) and the NPD (blue) strains with 1 mM IPTG after addition of 400 μg/ml 6-APA at time 0 (solid lines). Control cultures received no 6-APA (dashed lines). As another control, NPD without IPTG is also shown (black). (**B**) Simulated growth dynamics of PAD (red) and the NPD (blue) strains following 6-APA treatment ($a(0) = 5.5$). $\beta_1 = 0.04$ and 0 were used for PAD and the NPD strains, respectively, and $\beta_2 = 5.5$ was used. (**C**) Simulated growth of PAD (red) and the NPD (blue) strains following 6-APA treatment ($a(0) = 5.5$) as a function of public-good production (solid lines). The PAD strain is fitter only when coupled with sufficiently fast production of public good (red zone; $\beta_2 > 3.6$). Without 6-APA treatment, both strains reach the same high density (dotted lines). Cell densities at $\tau = 20$ are shown. (**D**) Growth of PAD (red) and the NPD (blue) strains following 400 μg/ml 6-APA treatment, at varying induction levels of BlaM modulated by IPTG (solid lines). Control cultures received no 6-APA (dotted lines). Cell densities (A_{600}) at the 24th hour are shown. Source data is available for this figure in the Supplementary Information.

death owing to the trade-off between programmed death and public-good release. If too drastic, programmed death cannot be sufficiently compensated for by the released public good. If too little, the amount of released public good will also be low and the population is unable to deal with the stress within the time frame of interest. Indeed, our model predicts an optimal degree of programmed death (as modulated by β_1, E synthesis rate; Figure 4A). We note that the emergence of the optimal death rate is critically dependent on temporal dynamics (Supplementary Figure S5a). The optimality emerges only after sufficient time; during the initial period, the bacterial density decreased monotonically with an increasing programmed death rate by the E protein.

Interestingly, the optimal degree of programmed death increases as the rate of public-good generation (β_2) is increased. When public-good generation is too slow ($\beta_2 < 3.3$), any programmed death is detrimental to the overall population because the amount of public good released is too small to cause substantial population recovery within the time frame of interest. For sufficiently fast public-good production ($\beta_2 \geqslant 3.3$), the optimal degree of programmed death increases with the rate of public-good generation: that is, it is better to die faster if the public good is being released faster (per cell).

This can be understood by considering the temporal dynamics of the system. In response to 6-APA, cells start to express the *E* gene and undergo a 'death phase'. The cell death then releases BlaM, and 6-APA concentration starts to drop. When 6-APA is sufficiently reduced, cell density enters its 'recovery phase'. Now consider two strategies, slow death and fast death. When public-good production rate is low ($\beta_2 = 3.3$), the duration of the recovery phase is relatively short owing to slow removal of 6-APA (Figure 4B, Supplementary Figure S5b). This makes fast death less advantageous despite the fact that it enables the population to enter the recovery phase earlier with greater recovery rate (Supplementary Figure S5b). When the public-good production rate is high ($\beta_2 = 5$), however, the duration of the recovery phase becomes relatively long. Now the fast growth rate in the recovery phase becomes more advantageous, making fast death a better strategy (Figure 4C). In other words, the increased public-good production renders more benefit for fast death than slow death owing to the nonlinearity of the system. We note that at sufficiently fast public-good production, the cost of drastic initial death can outweigh the benefit: a moderate degree of programmed death can release sufficient public good to neutralize 6-APA. As a result, the optimal death rate slightly decreases (Figures 4A, $\beta_2 > 5.5$). At the same time, however, higher public-good production rates result in overall elevation of growth, leading to an insensitive dependence of cell density on the death rate around the optimum (Figure 4A, inset).

These intricate dynamics highlight the complexity of the cost–benefit trade-off in programmed death in the temporal domain. They also underscore the need to use a kinetic model to capture the trade-off; this aspect is also evidenced by the requirement for sufficiently long growth duration for the emergence of optimality in death rate (Supplementary Figure S5a). We also note that the predicted optimality above is relevant for clonal populations. In mixed populations, the

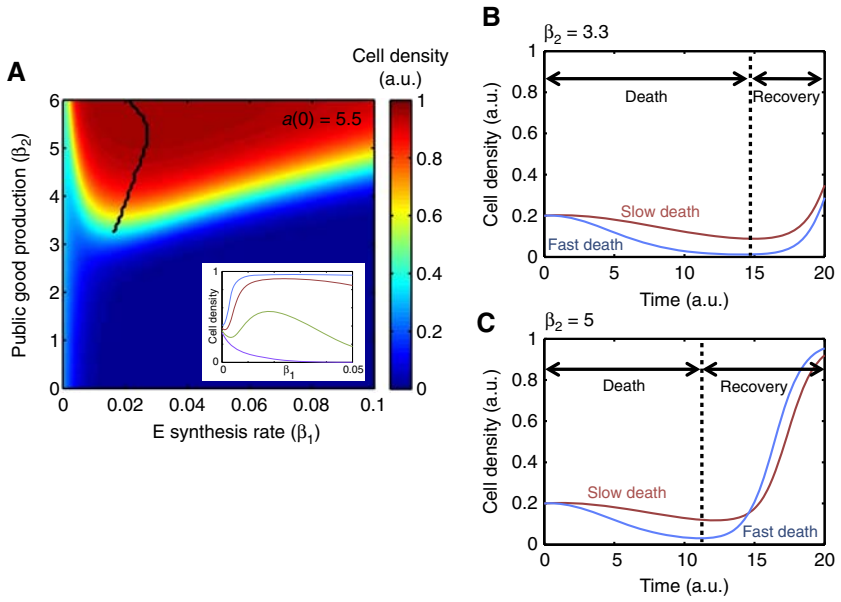

Figure 4 Predicted optimality in programmed death. (**A**) Simulated fitness landscape with respect to the E synthesis rate (β_1; x axis) and the public-good production rate (β_2; y axis) after 6-APA treatment ($a(0) = 5.5$). An optimal β_1 value shifts toward lower value as public-good production decreases (solid line). Inset: slices of the landscape along the x axis with different rates of public-good production (from blue to purple, $\beta_2 = 5.5$, 4.5, 3.5, and 2.5). Cell densities at $\tau = 20$ are shown. (**B**) Simulated population dynamics with low public-good production rate ($\beta_2 = 3.3$). 6-APA was added at time 0 and the following growth dynamics of population with either relatively high (blue; $\beta_1 = 0.03$) or low E synthesis rate (red; $\beta_1 = 0.01$) are shown. The fast-death population starts to recover after around time 14. (**C**) Simulated population dynamics with high public-good production rate ($\beta_2 = 5$). The fast-death population starts to recover after around time 11, which is earlier than the case in (B). The same β_1 values were used as in (B).

optimal degree of programmed death will likely be different and depend on the specific population structure (Ackermann *et al*, 2008; Chuang *et al*, 2009) (see Supplementary Text and Supplementary Figure S5c for further analysis and discussion).

To test the predicted optimality in the E synthesis rate, we created variants of the PAD circuit, termed iPAD (intermediate-level PAD), by attenuating the strength of ribosome-binding site (RBS) of the *E* gene. Modulating translation as opposed to transcription likely maintains activation characteristics of P_{ampC} in response to 6-APA (e.g., dose–response curve). Upon 6-APA treatment, all the variants exhibited intermediate degrees of lysis, which were greater than that by the NPD strain but less than that by the PAD strain (Figure 5A; Supplementary Figure S6a). We repeated the experiment shown in Figure 3A using iPAD strains to obtain a fitness landscape. At 0.031 mM IPTG, neither PAD strain nor iPAD strains did better than NPD, suggesting that altruistic death was not sufficiently beneficial. However, at 0.063 mM IPTG, we found the optimum at iPAD1 strain, the lowest degree of programmed death (Figure 5B, light blue line). As the IPTG concentration was increased, the optimum shifted to higher degrees of programmed death, confirming the model prediction (Figure 5B). We note that the further increase in BlaM expression by arabinose resulted in a flat landscape (Supplementary Figure S6b), consistent with model prediction (Figure 4A, inset).

The source of the observed optimality is the interdependency of cost and benefit in public-good release (i.e., increased lysis releases more public good). We note that recent studies (Gore *et al*, 2009; Chuang *et al*, 2010) also modulated the cost of public-good release in a synthetic, secretion-based cooperation system. However, this interdependency was absent because the cost was not directly tied to public-good release (modulation of cost was realized by using an arginine auxotroph and changing arginine concentration in the growth medium). Also, as noted in the modeling section (Supplementary Figure S5a), the emergence of the optimal programmed death rate depended on temporal dynamics (Supplementary Figure S6c).

Programed altruistic death and Eagle effect

As the degree of environmental stress in natural systems may vary (e.g., different levels of immune response in different hosts or different doses of antibiotic treatment), it is also important to test the response of our synthetic system to different doses of 6-APA. For a fixed β_2, our model predicts that growth of strains with small E synthesis rates ($\beta_1 < 0.006$) should monotonically decrease with increasing doses of 6-APA (Figure 6A). In contrast, strains with faster E synthesis ($\beta_1 \geqslant 0.006$) should exhibit non-monotonic dependence: for instance, at $\beta_1 = 0.04$, cell growth first decreases until $a = 0.4$, increases with further increase in 6-APA until $a = 5.25$, after which it starts to decrease again (Figure 6A, inset).

Consistent with these model predictions, we observed a non-monotonic dose response for PAD strains with relatively higher degree of lysis (Figure 6B). The iPAD3 and iPAD4 strains had higher density at 400 μg/ml 6-APA than at 200 μg/ml 6-APA; both the iPAD4 and the PAD strains had higher densities at 200 μg/ml 6-APA than at 100 μg/ml 6-APA. Given its foundation on altruistic death, the non-monotonic dose response appears only after sufficiently long growth duration (Supplementary Figure S7). When observed at earlier times, bacterial density decreased monotonically with an increasing 6-APA concentration.

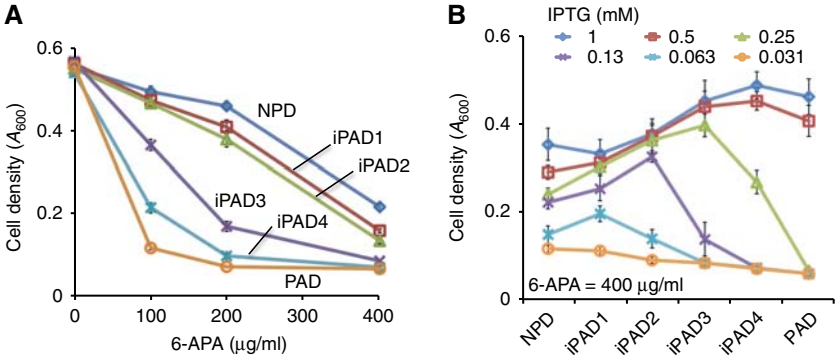

Figure 5 Experimental test of optimal death rates. (**A**) Variants of PAD with varying programmed death rates. Cultures of PAD variants (iPAD1 through iPAD4) as well as the original PAD and NPD strains were subject to various concentrations of 6-APA treatments without BlaM induction. Cell densities at 3-h time point after the 6-APA treatment are shown. These results indicate that the several strains can be ranked by programmed death rate as follows: NPD < iPAD1 < iPAD2 < iPAD3 < iPAD4 < PAD. (**B**) Verification of tunable optimality in death rates. Experiment was performed as described in Figure 3A. The constructs were listed in the order of increasing degree of lysis as determined in (A). Rates of BlaM expression were modulated by IPTG. Source data is available for this figure in the Supplementary Information.

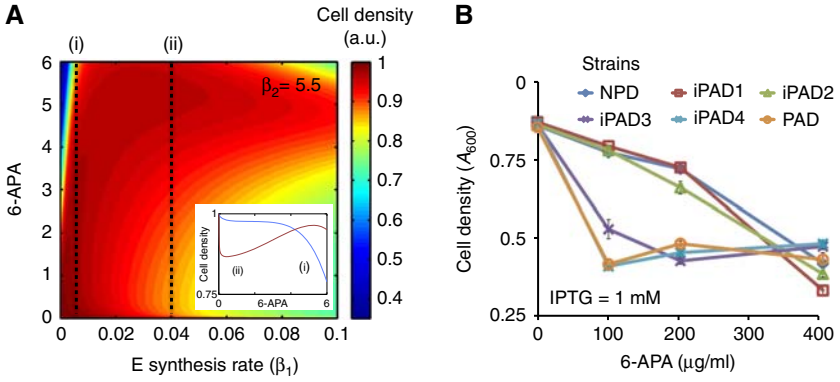

Figure 6 Eagle effect by altruistic death. (**A**) Simulated fitness landscape with respect to the E synthesis rate (β_1; x axis) and the stress level ($a(0)$; y axis) for $\beta_2 = 5.5$. For $\beta_1 < 0.06$, growth decreases monotonically with an increasing 6-APA dose ((i); blue line in inset ($\beta_1 = 0.005$)); otherwise, growth exhibits non-monotonic dependence ((ii); red line in inset ($\beta_1 = 0.04$)). Cell densities at $\tau = 20$ are shown. (**B**) Experimental test of (A). Experiment was performed as described in Figure 3A with the PAD variants treated with different concentrations of 6-APA and 1 mM IPTG. For the following pairs, cell densities treated with a higher 6-APA concentration were significantly greater than those treated with a lower 6-APA concentration ($P < 0.001$): 100 and 200 μg/ml 6-APA for PAD and iPAD4, and 200 and 400 μg/ml 6-APA for iPAD3 and iPAD4. Source data is available for this figure in the Supplementary Information.

A critical determinant for the generation of the non-monotonic dose response is the intrinsic negative feedback in the circuit: antibiotic-mediated cell lysis can lead to faster antibiotic degradation, and potentially faster population recovery. This logic can be readily realized in natural settings. One example is the treatment of bacteria expressing the wild-type beta-lactamase, Bla (i.e., periplasmic form). These bacteria may be moderately susceptible to a beta-lactam antibiotic. At a sufficiently high antibiotic dose, some cells will lyse and release their beta-lactamase. Released Bla will be more effective in degrading antibiotic than the native periplasmic Bla as it gains access to the higher antibiotic concentration in the culture than in the periplasm (Nagano and Nikaido, 2009). Therefore, the dynamics of these bacteria in response to antibiotic treatment will follow the same basic logic as captured by our circuit. As such, these bacteria may also exhibit non-monotonic response to increasing antibiotic dose. To test this idea, we replaced the BlaM in PAD with its wild-type counterpart Bla, which is periplasmic, to obtain PADbla. Consistent with our expectation, we observed non-monotonic dose responses when Bla production was moderately induced by 0.11 and 0.037 mM IPTG (Figure 7, Supplementary Figure S8). This result suggests that the logic captured by our circuit is generally applicable and could account for the 'Eagle effect', a counter-intuitive phenomenon where bacteria appear to grow better when treated with higher antibiotic concentrations.

Discussion

Programmed death has long been known in multicellular organisms, such as apoptosis, where cells are programmed to die for proper tissue development or prevention of cancerous cell growth. In this case, programmed death is critical for overall functionality of the individuals. Likewise, programmed death is involved in diverse aspects in bacterial physiology, including bacterial pathogenesis and stress response. In this context, the need to explain its existence has led to the proposal to consider programmed death as a social trait and, more specifically, an ultimate form of cooperation. This idea, however, has suffered from lack of explicit and thorough experimental analysis and has thus remained as a major problem in biology. To this end, our synthetic system provides

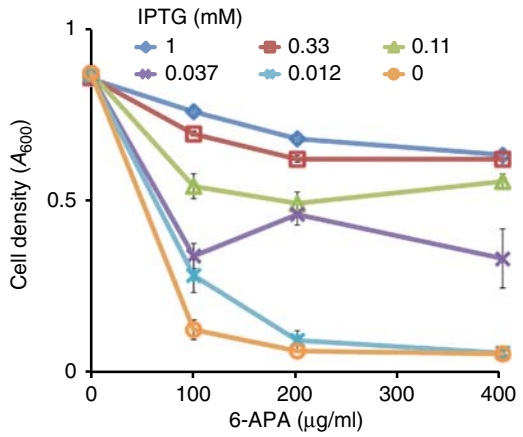

Figure 7 Responses of a Bla-expressing PAD strain (PADbla) to increasing 6-APA concentrations. Experiment was done similarly to Figure 6B except the PADbla was used. For the following pairs, cell densities treated with a higher 6-APA concentration were significantly greater than those treated with a lower 6-APA concentration ($P<0.001$): 100 and 200 μg/ml 6-APA for 0.037 mM IPTG, and 200 and 400 μg/ml 6-APA for 0.11 mM IPTG. The error bar for the condition with 0 mM IPTG and 400 μg/ml 6-APA is s.d. of seven replicates while those for other conditions are from eight replicates done over two independent experiments. Source data is available for this figure in the Supplementary Information.

a well-defined platform to address this problem, and unequivocally demonstrates the conditions where altruistic death becomes advantageous at the population level.

First, we found that public-good release following programmed death needs to be sufficiently high and would be maladaptive otherwise (Figure 3D). This idea is consistent with the observation that lysis capability of a wild-type lab strain of *S. pneumoniae* is reduced compared with its clinical isolate (Guiral *et al*, 2005). Intuitively, lysis is unlikely to provide any benefit under laboratory growth conditions because the released public good, pneumolysin, is a virulence factor that targets a variety of host functions, such as immune response. In the absence of such benefit, laboratory culturing of *S. pneumoniae* should lead to reduced lysis. Second, we showed that there exists an optimal degree of programmed death that depends on the amount of public-good release (Figure 5B). Also, the density at which programmed death is triggered has to be high enough for altruistic death to be advantageous (Supplementary Figure S3). These results provide an intuitive explanation for the regulation of programmed death observed in *E. coli*. In the *mazEF* module, the degree of programmed death is regulated by cell density through an extracellular peptide signal (Kolodkin-Gal *et al*, 2007). The degree of programmed death is much smaller at a low cell density than at a high density, indicating selection for fine-tuning of the degree of programmed death depending on the amount of public-good production.

From a practical perspective, it is increasingly recognized that bacterial social traits can serve as potential targets for antimicrobial treatment (Hentzer and Givskov, 2003; Andre and Godelle, 2005; Brown *et al*, 2009; Swem *et al*, 2009); thus, a better understanding of evolutionary aspects of bacterial social behaviors (including programmed death) can provide valuable insights for successful clinical intervention of bacterial infections (Köhler *et al*, 2010). For instance, there are at least two ways to reduce the 'benefit' of altruistic death: inhibiting occurrence of programmed death by interfering with its upstream signaling pathway, and inhibiting public-good production while letting programmed death be triggered. The latter would likely be a better intervention strategy because the bacterial population would still pay the cost (i.e., programmed death) without benefiting from it (analogous to PAD strain with very low or no BlaM production). Also it is worth noting that bacterial social behaviors have an important role in antibiotic resistance; a recent study revealed that a small number of resistant mutants can, at a fitness cost to themselves, provide protection to more drug-sensitive cells, thereby enhancing the survival of the total population (Lee *et al*, 2010). By providing direct experimental evidence for the circumstances of the advantage of altruistic death, our study constitutes an important step toward studying its evolutionary dynamics and potential intervention strategies.

A next step is to study the dynamics of altruistic death in mixed populations to examine other factors that are important for the evolution of costly cooperative traits (Fletcher and Doebeli, 2009). Conceptually, the condition for altruistic traits to be evolutionarily favored can be described by the Hamilton's rule (Hamilton, 1964a, b), $br>c$, where b and c, represent 'benefit' and 'cost' of altruistic traits whereas r measures 'relatedness' between individuals. Hamilton's rule indicates that higher relatedness, larger benefit, and lower cost favor evolution of altruistic traits. In this regard, previous studies experimentally illustrated that strong population bottleneck leads to higher r (Chuang *et al*, 2009). Our additional modeling analysis of mixed population (Supplementary Text) indeed showed that altruistic death (i.e., $\beta_1>0$) could be evolutionarily maintained when there is a strong population bottleneck (Supplementary Figure S5c). Also, it has been shown that a well-mixed non-clonal population can spatially segregate into clonal patches through simple surface growth (Hallatschek *et al*, 2007), suggesting a mechanism to generate a high level of assortment in nature. While r depends only on population structure, b and c often have complex, non-intuitive dependence on systems parameters (Chuang *et al*, 2010). Our modeling analysis of competition of NPD ($\beta_1=0$) and PAD ($\beta_1>0$) indeed illustrated this complexity under a simple population structure with relatively high r (Supplementary Figure S9). In particular, we found that PAD can outcompete NPD in a relatively narrow range of β_2 (i.e., public-good production). A close examination revealed that b shows a biphasic behavior while c monotonically increases for this range of β_2, satisfying Hamilton's rule only for a small range of β_2 (Supplementary Figure S9c, d). Altruistic death can potentially be favored by direct coupling to a benefit. For example, in the spore formation of social amoeba, *Dictyostelium discoideum*, the gene that leads to suicide also confers competitive advantage during spore formation. When mixed, a mutant lacking this gene avoids suicide but is eventually outcompeted by wild-type cells (Foster *et al*, 2004). Such pleiotropy makes the loss of 'suicide gene' costly and could therefore stabilize altruistic death. Also important is the regulation of programmed death. Cell-density-dependent death (Kolodkin-Gal *et al*, 2007) and bistable regulation that generates phenotypically distinct dying and non-dying subpopulations (Reuven and Eldar, 2011) may help

evolution of altruistic death by preventing unnecessary death. Although altruistic death is generally prone to exploitation by non-altruistic individuals, the combination of abovementioned mechanisms may allow its evolution.

Equally important, our results established a new mechanistic explanation for the Eagle effect (Figures 6 and 7), which has been observed in antibiotic treatment of a variety of microbial species both *in vivo* (Eagle and Musselman, 1948; Lorian *et al*, 1979; Ikeda *et al*, 1987; Ikeda and Nishino, 1988; Lewin *et al*, 1991; Kondo *et al*, 2001; McKay *et al*, 2009) and *in vitro* (Ikeda *et al*, 1990). Two explanations for the Eagle effect have been proposed: reduced antimicrobial activity of the drug itself at high concentration (Nishino and Nakazawa, 1976; Lewin *et al*, 1991) and induction of resistance mechanisms at high antibiotic concentration (Ikeda *et al*, 1987; Ikeda and Nishino, 1988; Kondo *et al*, 2001). Our results suggest another mechanism: the release of beta-lactamase into environment through cell lysis. By the same logic, any cellular components that are released by cell lysis and able to counteract the antibiotic could potentially cause the Eagle effect. Our mechanism provides a link between two apparently unrelated phenomena, altruistic death and the Eagle effect; it has implications for effective design of antibiotic treatment protocols.

Materials and methods

Strains, growth media, and chemicals

E. coli strains constructed and used in this study are summarized in Supplementary Table S1. *E. coli* strain SN0301 (*ampD1*, *ampA1*, *ampC8*, *pyrB*, *recA*, and *rpsL*) (Lindberg *et al*, 1987) was used as a parental strain of other strains. The *ampD1* mutation enables hyper-induction of P_{ampC} in response to beta-lactam antibiotics (Lindberg *et al*, 1987). Unless otherwise noted, LBKM medium (10 g tryptone, 5 g yeast extract, 7 g KCl, and 100 mM MOPS) (Balagaddé *et al*, 2005) buffered at pH 7.0 was used for cell growth assays. pH was adjusted by adding 5 M KOH. For every experiment, × 100 6-APA solution was prepared fresh by dissolving it in 1 M HCl. Spectinomycin (50 μg/ml), kanamycin (50 μg/ml), and chloramphenicol (20 μg/ml) were used for plasmid maintenance. Appropriate concentrations of IPTG were added to growth medium when applicable.

Plasmids

All plasmids were constructed using standard molecular biology techniques and summarized in Supplementary Table S1. Briefly, the public-good module, pBlaM, was constructed by PCR-amplifying *bla* gene from pSND-1 (gift from Dr Ron Weiss) without first 66 base pairs and inserting it under $P_{lac/ara-1}$ of pPROLar.A122 (Clonetech). A start codon (atg) for the truncated *bla* was also included during the PCR step, resulting in *blaM*. pBla was constructed in the same way except that the wild-type *bla* gene was inserted instead of *blaM*. The suicide module, pCSaE500, was constructed based on pTS1 (Sohka *et al*, 2009), which harbors *gfp* and *tetC* under ampR-P_{ampC} cassette from *Citrobacter freundii*. *gfp* and *tetC* were replaced with *E* gene, which was PCR amplified from pRY100 (Roof *et al*, 1997). *E* gene was simply removed by restriction digestion and blunt-end ligation to obtain pCSa for NPD. To construct iPAD strains, we used a recently developed algorithm, RBS Calculator (Salis *et al*, 2009), to design appropriate RBS sequences of *E* gene (Supplementary Table S2). pCSaE500, a suicide module of the original PAD, has RBS strength of 500 (arbitrary unit in the algorithm) and the four variants have RBS strength of either 375 or 450. As the algorithm is usually accurate within a twofold range, the resulting variants still exhibit differential RBS strength. GFP reporter construct for P_{ampC} activity, pCSaGFP, was constructed by replacing *E* gene in the suicide module with *gfpmut3*. RBS strength for GFP was also reduced to minimize leaky expression of GFP.

Growth experiment

Cells transformed with appropriate plasmids were inoculated into Luria–Bertani (LB) medium from single colonies and grown at 37 °C overnight for 18–19 h. The overnight cultures were diluted by 200-fold into LBKM medium (10 g tryptone, 5 g yeast extract, and 7 g KCl per liter, and 100 mM 3-(*N*-morpholino) propanesulfonic acid (MOPS), buffered at pH 7.0 by adding 5 M KOH) and 200 μl cultures were grown in 96-well microplates at 37 °C in an orbital shaker shaken at 400 r.p.m. Unless otherwise indicated, appropriate concentration of 6-APA was added after 4.5 h (A_{600} of 0.15–0.2). Throughout the experiment, two sealing membranes were used to reduce evaporation while allowing aerobic growth: the microplates were sealed first with AeraSeal (Excel Scientific) and then Breathe-Easy membrane (Diversified Biotech). This combination of membranes has been used as a way to achieve both low medium evaporation and high bacterial growth (Börner *et al*, 2007). Absorbance at 600 nm (A_{600}) was recorded using Victor 3 plate reader (Perkin Elmer). After each measurement, the two membranes were applied to the plate as described above. Unless otherwise noted, error bars in each figure are s.d. of 8 replicates (four technical replicates × two independent experiments).

P_{ampC} reporter assay

If BlaM effectively degrades 6-APA and prevents cell-wall damage when present in the cytoplasm, then BlaM expression alone should decrease the induction of P_{ampC} reported by GFP. However, GFP expression did not show significant difference between with (blue, no IPTG) and without (green, 1 mM IPTG) BlaM induction, which indicates that BlaM expression does not prevent cell-wall damage by 6-APA (Figure 2A). In contrast, when native beta-lactamase, *bla*, was expressed, which is known to effectively protect cell from 6-APA action, GFP expression decreased significantly (Figure 2A). P_{ampC} assay strains carrying pBlaM or pBla were grown as described in the previous section with or without 1 mM IPTG. GFP was induced using 50 μg/ml 6-APA and samples were taken 2 h after 6-APA treatment and subject to flow cytometry analysis.

Protection assay

Overnight culture of PAD strain was diluted by 200-fold into LBKM media and grown in culture tubes with or without 1 mM IPTG. When the A_{600} reached 0.15–0.2, these cultures were treated with or without 400 μg/ml 6-APA. After 5 h, these cells were spun down and supernatant was filtered by 0.2 μm cellulose-acetate membrane. BlaM activity in the supernatant was assayed by growth of a 6-APA-sensitive strain (Supplementary Table S1, assay strain) after 12 h in the supernatant in a 96-well plate covered with mineral oil to prevent evaporation.

Summary of mathematical modeling

As detailed in Supplementary Text, a non-dimensionalized ODE model for cell density (n), E protein (x), extracellular BlaM (b), and 6-APA (a) was developed to analyze the system's behaviors:

$$\frac{dn}{d\tau} = gn - ln \tag{1}$$

$$\frac{dx}{d\tau} = \beta_1\left(\frac{a}{\sigma_2 + a} + \frac{x}{\sigma_3 + x}\right) - (\gamma_2 + g)x \tag{2}$$

$$\frac{db}{d\tau} = \beta_2 ln - \gamma_3 b \tag{3}$$

$$\frac{da}{d\tau} = -\frac{ba}{1 + a} \tag{4}$$

$$g = (1 - n)\frac{\sigma_1}{\sigma_1 + a} \tag{5}$$

$$l = \frac{\gamma_1(\omega a + x)}{1 + (\omega a + x)} \tag{6}$$

where g and l represent cell growth rate and lysis rate, respectively. We did not consider the growth effect of E protein as it appears to be minor (Supplementary Figure S1) although incorporating this effect does not change our conclusions qualitatively. Experimentally, modifying RBS corresponds to changing β_1; and changing IPTG concentration corresponds to changing β_2. Initial conditions of $n(0) = 0.2$, $x(0) = 0$, $b(0) = 0$, and $a(0) = 0$–5.5 were used for all the simulation results except for Figure 3B where $n(0) = 0.0058$ to capture initial growth before 6-APA treatment. The description and values of the parameters are summarized in Supplementary Table S3. See Supplementary Text for further details of model development.

Supplementary information

Supplementary information is available at the *Molecular Systems Biology* website (www.nature.com/msb).

Acknowledgements

We thank S West for insightful comments on an early version of the manuscript, M Ostermeier for strain SN0301 and plasmid pTS1, and R Weiss for plasmid pSND-1. This work was supported by the National Institutes of Health (1P50-GM081883, 1R01-GM098642), a National Science Foundation CAREER award (LY, CBET-0953202), a DuPont Young Professorship (LY), and a David and Lucile Packard Fellowship (LY). NEB was supported by a Career Award at the Scientific Interface from Burroughs Wellcome Fund and by the National Institutes of Health through the NIH Director's New Innovator Award Program (DP2-OD-008654).

Author contributions: YT conceived the research, designed and performed both modeling and experimental analyses, interpreted the results, and wrote the manuscript. AP assisted in experimental analyses, data interpretation, and manuscript revisions. NEB assisted in modeling the analyses, and interpreting the results and manuscript revisions. LY conceived the research, assisted in research design and data interpretation, and wrote the manuscript. All authors approved the manuscript.

Conflict of interest

The authors declare that they have no conflict of interest.

References

Acar M, Mettetal JT, van Oudenaarden A (2008) Stochastic switching as a survival strategy in fluctuating environments. *Nat Genet* **40:** 471–475

Ackermann M, Stecher B, Freed NE, Songhet P, Hardt W-D, Doebeli M (2008) Self-destructive cooperation mediated by phenotypic noise. *Nature* **454:** 987–990

Aizenman E, EngelbergKulka H, Glaser G (1996) An *Escherichia coli* chromosomal 'addiction module' regulated by 3′,5′-bispyrophosphate: a model for programmed bacterial cell death. *Proc Natl Acad Sci USA* **93:** 6059–6063

Allesen-Holm M, Barken KB, Yang L, Klausen M, Webb JS, Kjelleberg S, Molin S, Givskov M, Tolker-Nielsen T (2006) A characterization of DNA release in *Pseudomonas aeruginosa* cultures and biofilms. *Mol Microbiol* **59:** 1114–1128

Andre J, Godelle B (2005) Multicellular organization in bacteria as a target for drug therapy. *Ecol Lett* **8:** 800–810

Balagaddé FK, You L, Hansen CL, Arnold FH, Quake SR (2005) Long-term monitoring of bacteria undergoing programmed population control in a microchemostat. *Science* **309:** 137–140

Berry AM, Yother J, Briles DE, Hansman D, Paton JC (1989) Reduced virulence of a defined pneumolysin-negative mutant of *Streptococcus pneumoniae*. *Infect Immun* **57:** 2037–2042

Börner J, Buchinger S, Schomburg D (2007) A high-throughput method for microbial metabolome analysis using gas chromatography/mass spectrometry. *Anal Biochem* **367:** 143–151

Broome-Smith JK, Spratt BG (1986) A vector for the construction of translational fusions to TEM beta-lactamase and the analysis of protein export signals and membrane protein topology. *Gene* **49:** 341–349

Brown SP, West SA, Diggle SP, Griffin AS (2009) Social evolution in micro-organisms and a Trojan horse approach to medical intervention strategies. *Philos Trans R Soc Lond, B, Biol Sci* **364:** 3157–3168

Cascales E, Buchanan SK, Duché D, Kleanthous C, Lloubès R, Postle K, Riley M, Slatin S, Cavard D (2007) Colicin biology. *Microbiol Mol Biol Rev* **71:** 158–229

Chuang JS, Rivoire O, Leibler S (2009) Simpson's paradox in a synthetic microbial system. *Science* **323:** 272–275

Chuang JS, Rivoire O, Leibler S (2010) Cooperation and Hamilton's rule in a simple synthetic microbial system. *Mol Syst Biol* **6:** 398

Eagle H, Musselman AD (1948) The rate of bactericidal action of penicillin *in vitro* as a function of its concentration, and its paradoxically reduced activity at high concentrations against certain organisms. *J Exp Med* **88:** 99–131

Ellermeier CD, Hobbs EC, Gonzalez-Pastor JE, Losick R (2006) A three-protein signaling pathway governing immunity to a bacterial cannibalism toxin. *Cell* **124:** 549–559

Everett MJ, Chopra I, Bennett PM (1990) Induction of the *Citrobacter freundii* group I beta-lactamase in *Escherichia coli* is not dependent on entry of beta-lactam into the cytoplasm. *Antimicrob Agents Chemother* **34:** 2429–2430

Fletcher JA, Doebeli M (2009) A simple and general explanation for the evolution of altruism. *Proc Biol Sci* **276:** 13–19

Foster KR, Shaulsky G, Strassmann JE, Queller DC, Thompson CRL (2004) Pleiotropy as a mechanism to stabilize cooperation. *Nature* **431:** 693–696

Gardner A, Kümmerli R (2008) Social evolution: this microbe will self-destruct. *Curr Biol* **18:** R1021–R1023

Gardner A, West SA, Buckling A (2004) Bacteriocins, spite and virulence. *Proceed Biol Sci/R Soc* **271:** 1529–1535

Gore J, Youk H, van Oudenaarden A (2009) Snowdrift game dynamics and facultative cheating in yeast. *Nature* **459:** 253–256

Guiral S, Mitchell TJ, Martin B, Claverys J-P (2005) Competence-programmed predation of noncompetent cells in the human pathogen *Streptococcus pneumoniae*: genetic requirements. *Proc Natl Acad Sci USA* **102:** 8710–8715

Hallatschek O, Hersen P, Ramanathan S, Nelson DR (2007) Genetic drift at expanding frontiers promotes gene segregation. *Proc Natl Acad Sci USA* **104:** 19926–19930

Hamilton WD (1964a) The genetical evolution of social behaviour. I. *J Theor Biol* **7:** 1–16

Hamilton WD (1964b) The genetical evolution of social behaviour. II. *J Theor Biol* **7:** 17–52

Haraga A, Ohlson MB, Miller SI (2008) Salmonellae interplay with host cells. *Nat Rev Microbiol* **6:** 53–66

Hazan R, Sat B, Engelberg-Kulka H (2004) *Escherichia coli* mazEF-mediated cell death is triggered by various stressful conditions. *J Bacteriol* **186:** 3663–3669

Hentzer M, Givskov M (2003) Pharmacological inhibition of quorum sensing for the treatment of chronic bacterial infections. *J Clin Invest* **112:** 1300–1307

Hirst RA, Kadioglu A, O'callaghan C, Andrew PW (2004) The role of pneumolysin in *Pneumococcal pneumonia* and *meningitis*. *Clin Exp Immunol* **138:** 195–201

Ikeda Y, Fukuoka Y, Motomura K, Yasuda T, Nishino T (1990) Paradoxical activity of beta-lactam antibiotics against *Proteus vulgaris* in experimental infection in mice. *Antimicrob Agents Chemother* **34:** 94–97

Ikeda Y, Nishino T (1988) Paradoxical antibacterial activities of beta-lactams against *Proteus vulgaris*: mechanism of the paradoxical effect. *Antimicrob Agents Chemother* **32:** 1073–1077

Ikeda Y, Nishino T, Tanino T (1987) Paradoxical antibacterial activity of cefmenoxime against *Proteus vulgaris*. *Antimicrob Agents Chemother* **31:** 865–869

Jacobs C, Frère JM, Normark S (1997) Cytosolic intermediates for cell wall biosynthesis and degradation control inducible beta-lactam resistance in gram-negative bacteria. *Cell* **88:** 823–832

Kerr B, Riley MA, Feldman MW, Bohannan BJM (2002) Local dispersal promotes biodiversity in a real-life game of rock-paper-scissors. *Nature* **418:** 171–174

Köhler T, Perron GG, Buckling A, van Delden C (2010) Quorum sensing inhibition selects for virulence and cooperation in *Pseudomonas aeruginosa*. *PLoS Pathogens* **6:** e1000883

Kolodkin-Gal I, Hazan R, Gaathon A, Carmeli S, Engelberg-Kulka H (2007) A linear pentapeptide is a quorum-sensing factor required for mazEF-mediated cell death in *Escherichia coli*. *Science* **318:** 652–655

Kondo N, Kuwahara-Arai K, Kuroda-Murakami H, Tateda-Suzuki E, Hiramatsu K (2001) Eagle-type methicillin resistance: new phenotype of high methicillin resistance under mec regulator gene control. *Antimicrob Agents Chemother* **45:** 815–824

Lee HH, Molla MN, Cantor CR, Collins JJ (2010) Bacterial charity work leads to population-wide resistance. *Nature* **467:** 82–85

Lewin CS, Morrissey I, Smith JT (1991) The mode of action of quinolones: the paradox in activity of low and high concentrations and activity in the anaerobic environment. *Eur J Clin Microbiol Infect Dis* **10:** 240–248

Lindberg F, Lindquist S, Normark S (1987) Inactivation of the ampD gene causes semiconstitutive overproduction of the inducible *Citrobacter freundii* beta-lactamase. *J Bacteriol* **169:** 1923–1928

Lorian V, Silletti RP, Biondo FX, De Freitas CC (1979) Paradoxical effect of aminoglycoside antibiotics on the growth of Gram-negative bacilli. *J Antimicrob Chemother* **5:** 613–616

Lutz R, Bujard H (1997) Independent and tight regulation of transcriptional units in *Escherichia coli* via the LacR/O, the TetR/O and AraC/I-1-I-2 regulatory elements. *Nucleic Acids Res* **25:** 1203–1210

McKay GA, Beaulieu S, Arhin FF, Belley A, Sarmiento I, Parr T, Moeck G (2009) Time-kill kinetics of oritavancin and comparator agents against *Staphylococcus aureus*, *Enterococcus faecalis* and *Enterococcus faecium*. *J Antimicrob Chemother* **63:** 1191–1199

Nagano K, Nikaido H (2009) Kinetic behavior of the major multidrug efflux pump AcrB of *Escherichia coli*. *Proc Natl Acad Sci USA* **106:** 5854–5858

Nedelcu AM, Driscoll WW, Durand PM, Herron MD, Rashidi A (2011) On the paradigm of altruistic suicide in the unicellular world. *Evolution* **65:** 3–20

Nishino T, Nakazawa S (1976) Bacteriological study on effects of beta-lactam group antibiotics in high concentrations. *Antimicrob Agents Chemother* **9:** 1033–1042

Reuven P, Eldar A (2011) Macromotives and microbehaviors: the social dimension of bacterial phenotypic variability. *Curr Opin Genet Dev* **21:** 759–767

Rice KC, Bayles KW (2003) Death's toolbox: examining the molecular components of bacterial programmed cell death. *Mol Microbiol* **50:** 729–738

Rice KC, Mann EE, Endres JL, Weiss EC, Cassat JE, Smeltzer MS, Bayles KW (2007) The cidA murein hydrolase regulator contributes to DNA release and biofilm development in *Staphylococcus aureus*. *Proc Natl Acad Sci USA* **104:** 8113–8118

Roof WD, Fang HQ, Young KD, Sun J, Young R (1997) Mutational analysis of slyD, an *Escherichia coli* gene encoding a protein of the FKBP immunophilin family. *Mol Microbiol* **25:** 1031–1046

Salis HM, Mirsky EA, Voigt CA (2009) Automated design of synthetic ribosome binding sites to control protein expression. *Nat Biotechnol* **27:** 946–950

Shou W, Ram S, Vilar JMG (2007) Synthetic cooperation in engineered yeast populations. *Proc Natl Acad Sci USA* **104:** 1877–1882

Sohka T, Heins RA, Phelan RM, Greisler JM, Townsend CA, Ostermeier M (2009) An externally tunable bacterial band-pass filter. *Proc Natl Acad Sci USA* **106:** 10135–10140

Song H, Payne S, Gray M, You L (2009) Spatiotemporal modulation of biodiversity in a synthetic chemical-mediated ecosystem. *Nat Chem Biol* **5:** 929–935

Stecher B, Robbiani R, Walker AW, Westendorf AM, Barthel M, Kremer M, Chaffron S, Macpherson AJ, Buer J, Parkhill J, Dougan G, von Mering C, Hardt W-D (2007) *Salmonella enterica* serovar typhimurium exploits inflammation to compete with the intestinal microbiota. *PLoS Biol* **5:** 2177–2189

Swem LR, Swem DL, O'Loughlin CT, Gatmaitan R, Zhao B, Ulrich SM, Bassler BL (2009) A quorum-sensing antagonist targets both membrane-bound and cytoplasmic receptors and controls bacterial pathogenicity. *Mol Cell* **35:** 143–153

Tanouchi Y, Pai A, You L (2009) Decoding biological principles using gene circuits. *Mol Biosyst* **5:** 695–703

West SA, Diggle SP, Buckling A, Gardner A, Griffins AS (2007) The social lives of microbes. *Annu Rev Ecol Evol S* **38:** 53–77